17th World Conference on Earthquake Engineering, 17WCEE
Sendai, Japan - September 13th to 18th 2020

Uncertainty Estimation of Servo-Hydraulic Dynamics for Real-Time Testing

C. Chen[1], C. Peng[2], C. Martinez[3], W. Xu[4] and K. Dy Cornejo[3]

[1] *Associate Professor, School of Engineering, San Francisco State University, chcsfsu@sfsu.edu*
[2] *Graduate research assistant, College of Civil Engineering, Shandong University, China, 958503343@qq.com*
[3] *Graduate research assistant, School of Engineering, San Francisco State University, cmartinez@mail.sfsu.edu*
[4] *Assistant professor, College of Civil Engineering, Southeast University, China, 1224418158@qq.com*
[5] *Graduate research assistant, School of Engineering, San Francisco State University, kcornej2@mail.sfsu.edu*

Abstract

Real-time hybrid simulation (RTHS) provides a cost-effective and efficient technique to enable seismic performance evaluation of large- and full-scale civil engineering structures. Servo-hydraulic actuators are often used in RTHS to impose desired displacements to specimens in laboratories and to maintain the boundary compatibility between substructures. Servo-hydraulic dynamics however introduces amplitude and phase errors in actuator response therefore presents a great challenge for RTHS. Various control strategies have been proposed and implemented to improve actuator tracking. Previous studies however often consider the servo-hydraulic system as deterministic while experimental results indicate otherwise due to different sources of uncertainties. This study utilizes the generalized likelihood uncertainty estimation (GLUE) method to estimate the uncertainties in servo-hydraulic dynamics. Probabilistic distribution and statistical moments are derived for parameters of a commonly used linearized servo-hydraulic model based on experimental results. The probabilistic model predictions are compared with those of the deterministic model as well as the experimental results. The GLUE method is shown to enable better prediction of actuator response through accounting for inherent uncertainties in servo-hydraulic system. The presented probabilistic analysis results can be further applied toward uncertainty analysis of RTHS for engineering research.

Keywords: Real-Time Hybrid Simulation, Uncertainty, Generalized Likelihood Uncertainty Estimation

1. Introduction

Hybrid simulation (HS) method provides an efficient integration between physical experiments and computational modeling. The critical and complex components of a structural system that may be difficult to model numerically are built in laboratories and tested as the experimental substructures while the rest of the structural system, generally simple to model and analyze, is numerically modeled as the analytical substructures. HS method therefore has attracted considerable interests in the past few decades [1-3] and has been extended to geographically distributed experimental substructures [4-5], and to real-time hybrid simulation (RTHS) [6-8] to account for rate-dependent behavior within experimental substructures. Through the integration of numerical modelling of analytical substructures and physical testing of experimental substructures, RTHS enables large- or full-scale tests in size limited structural laboratories to evaluate seismic performance of engineering structures with rate dependent devices [9]. During the developments for RTHS, servo-hydraulic dynamics have attracted significant attention from the hybrid simulation community [10-13]. A phenomenon often referred to as actuator is equivalent to negative damping and could deviate experimental results from actual structural responses, or even destabilize the entire test if not compensated properly. Different delay compensation methods therefore have been proposed and implemented for RTHS, such as the polynomial extrapolation method [14], the inverse compensation [8], the adaptive inverse control [15], and the adaptive model reference control [16].

Traditional HS and RTHS often assume that properties of the numerical substructures are deterministic. To account for inherent uncertainties within engineering structures, analytical substructures in HS and RTHS should be characterized as stochastic instead of deterministic [17-19]. To focus on uncertainties from structures and ground motions, these studies often ignored the servo-hydraulic system which however also presents additional source of uncertainty in RTHS. More recently, a RTHS benchmark problem [20] was presented to the community with the focus on the design of an effective displacement tracking controller. Uncertainties were introduced into the transfer function parameters of main components of the servo-hydraulic system to ensure robust stability and performance of the controller. Generally, two different approaches are often used for servo-hydraulic modeling, i.e., the first-principle modeling and the data-driven modelling. The first-principle modelling approach utilizes the understanding of servo-hydraulic system's physics to derive a mathematical representation. For example, Zhao *et al.* [21] studies the difference of using a first order and second order transfer function for the servo-valve used in the effective force testing studies at the University of Minnesota. An alternative for the first principle modeling is the data driven modeling approach, which builds relationships between input and output data without paying too much attention to the underlying processes. For example, Reinhorn *et al.* [22] used a pure delay to model the servo-hydraulic dynamics under the displacement control. In this study, the first-principle modeling of servo-hydraulic system is explored for its parameter uncertainties in real-time testing.

2. Simplified Modeling of Servo-Hydraulic Dynamics

When the fluid flow rate in an actuator is linearized about the origin, the coupling between the actuator dynamics and the physical specimen can be schematically represented in Fig. 1, where s is the Laplace variable. The linearized equation of hydraulic flow rate in a servo-hydraulic actuator in Fig. 1 can be mathematically expressed as

$$\dot{f} = \frac{2\beta}{V}\left(AK_q i - K_c f - A^2 \dot{x}_1\right) \tag{1}$$

where f, b, V, A, K_q, i, K_c and x_1 are actuator force, bulk modulus of the fluid, volume of the hydraulic actuator, piston area, valve flow gain, valve input, leakage coefficient and actuator displacement, respectively. Eq. (1) presents the dynamics of the force applied by the actuator to physical specimen. It can be observed from Fig. 1 and Eq. (1) that the dynamics of physical specimen directly impact the characteristics of the plant. When the physical specimen undergoes structural changes (such as stiffness changes due to nonlinear behavior) or is replaced by a different specimen, the overall servo-hydraulic dynamics change accordingly through the natural velocity feedback [20].

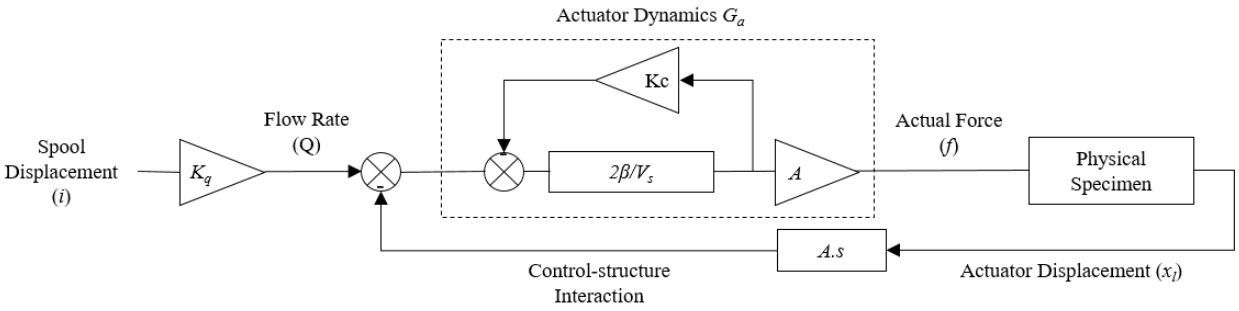

Fig. 1. Block diagram of an open-loop hydraulic actuator coupled with a physical specimen

Maghareh *et al.* [23] used a first order model for the servo-valve dynamics, and consolidate the nonlinear system of differential equations into a linear system with the following transfer function from external command (u) to actuator displacement (x_1)

$$G_{x_1,u} = \frac{n_0}{d_2 s^2 + d_1 s + d_0} \tag{2a}$$

where the coefficients of the numerator and the denominator are defined as $n_0 = a_1\beta_0$; $d_2 = k + a_2$; $d_1 = a_3 k + \beta_1 k + \beta_1 a_2$; and $d_0 = \beta_1 a_3 k + a_1\beta_0$, respectively; γ and β_1 denote a constant gain and servo-valve time constant, respectively. It can be observed that when there is no specimen, i.e., k=0, the static gain of Eq. (2a) is unity. The parameters associated with the servo-hydraulic transfer system are listed in Table 1.

Table 1. Hydraulic transfer system parameters

Parameter	Units	Component	Description
P	mA/m	Analog Controller	Controller proportional gain
γ	m/mA/sec	Servo-valve	Servo-valve gain
$1/\beta_1$	sec	Servo-valve	Servo-valve time constant
K_q	m^3/sec/m	Servo-valve	Valve flow gain
i	m	Servo-valve	Spool displacement
A	m^2	Hydraulic actuator	Piston area
K_c	m^3/sec/Pa	Hydraulic actuator	Leakage coefficient
V	m^3	Hydraulic actuator	Half the volume of the actuator
β	Pa	Hydraulic actuator	Effective bulk modulus of the fluid
Q	m^3/sec	Hydraulic actuator	Fluid flow rate into the actuator
x_1	m	Hydraulic actuator	Actuator displacement
f	N	Hydraulic actuator	Actuator force

Eq. (2a) can be revised as

$$G_{x_1,u} = \frac{{}^{n_0}/_{d_2}}{s^2 + {}^{d_1 s}/_{d_2} + {}^{d_0}/_{d_2}} \tag{2b}$$

To identify the four parameters in Eq. (2b), tests without specimen (k=0) and with simple linear elastic spring (k=250 kN/m) are conducted at the structural laboratory of Southeast University. Figure 2 shows the schematics and picture of the experimental setup. For both tests only the proportional (P) gain is used for the servo hydraulic PID controller. A sine sweep signal is selected as the command displacement with the

frequency increasing from 0 to 10 Hz in a duration of 60 seconds. Due to the limitation of hydraulic power supply, the amplitude of the sine sweep signal is set to 2 mm.

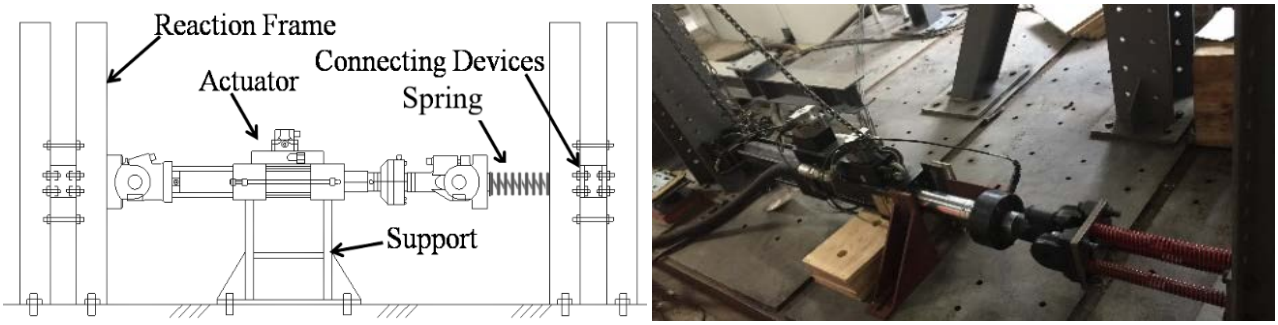

Figure 2. Experimental setup for servo-hydraulics identification: (a) schematics, (b) picture

Figures 3 and 4 show the comparison of measured and command displacements of tests with k=0 (i.e., free standing actuator) and k=250 kN/m, respectively. Different actuator tracking performance can be observed for the two tests in Figures 3(a) and 4(a). This again verifies that overall servo-hydraulic dynamics change accordingly for a different specimen. It can also be observed in Figures 4(b)~(d) that, compared with those of the free-standing actuator in Figures 3(b)~(d), the test with linear elastic spring has larger amplitude decay and larger phase delay with the increase of input frequency.

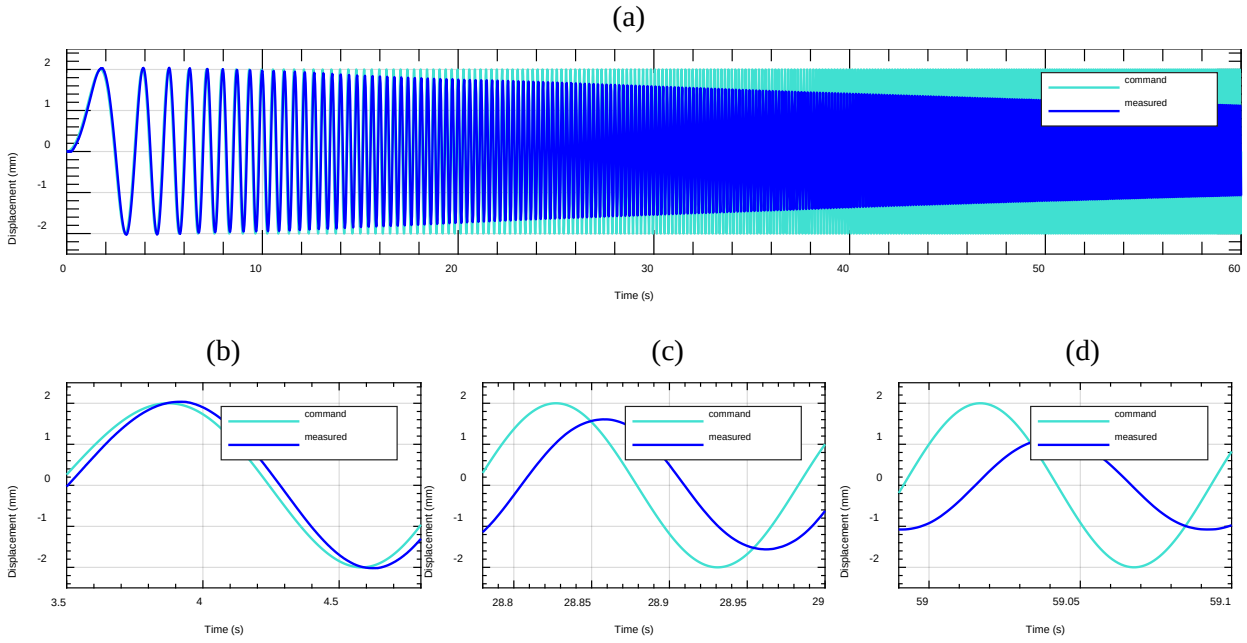

Figure 3. Comparison between the command and measured displacements for sine-sweep test with k=0: (a) time history; and close-up views for (b) 1Hz, (c) 5Hz, (d) 10Hz

Using the function *tfest* in Matlab [24], the transfer function in Eq. (2b) can be identified for the two tests, respectively, as

$$G_{x_1,u} = \frac{4609}{s^2+140s+4609} \tag{3a}$$

$$G_{x_1,u} = \frac{2208}{s^2+133s+2101} \tag{3b}$$

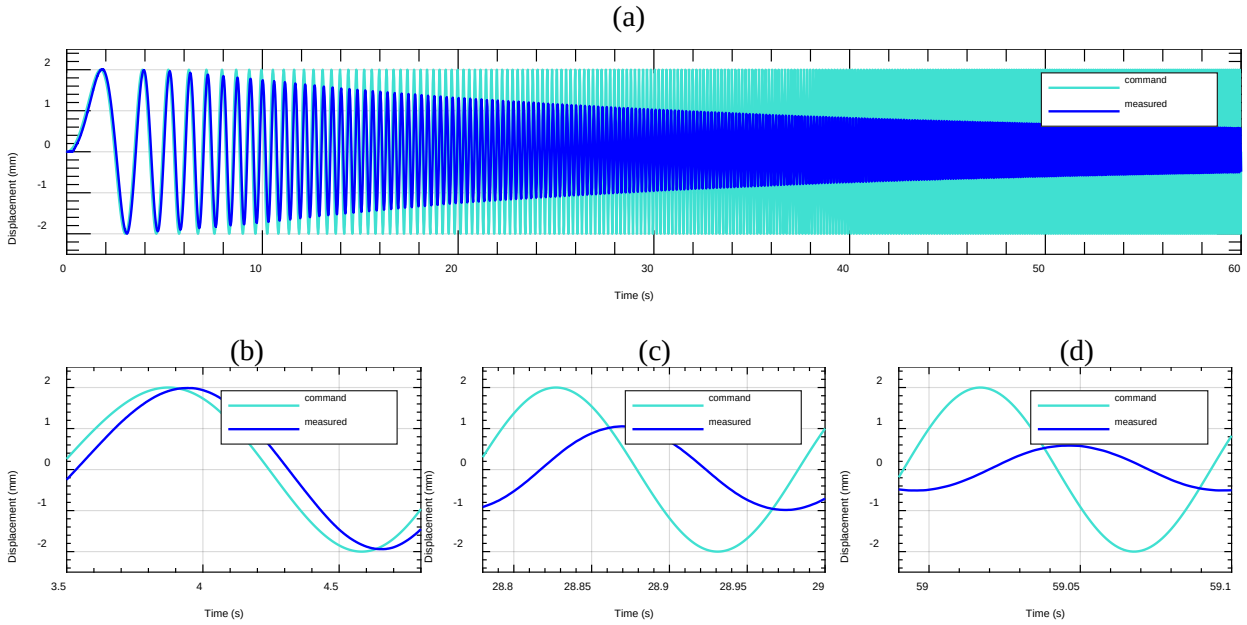

Figure 4. Comparison between the command and measured displacements for sine-sweep test with k=250kN/mm: (a) time history; and close-up views for (b) 1Hz, (c) 5Hz, (d) 10Hz

For the case of k=0, Eq. (3a) shows a static gain of 1.0, while Eq. (3b) shows a static gain of 1.05 for the case of k=250 kN/m. This larger static gain in Eq. (3b) than 1.0 can be attributed to the fact that only P gain is used for the servo-hydraulic controller during the tests. The individual values of the parameters are calculated and presented in Table 2. The two transfer functions in Eqs. (3a) and (3b) are referred to hereafter as deterministic models for the servo-hydraulic system in this study.

Table 2. Deterministic values of parameters

β_1 (N/s^2)	$\alpha_1\beta_0$ (N/ms^2)	α_2 (N/m)	α_3 (N·m)
128	1.01×10^9	2.42×10^5	0.06

3. Generalized Likelihood Uncertainty Estimation (GLUE)

The above process of identifying servo-hydraulic system parameters is often defined as inverse problem. In traditional inverse problems, researchers aim to obtain a set of optimal parameters to replicate the behavior of the engineering system under investigation. Root mean square (RMS) errors and evolutionary algorithms are commonly applied such as particle swamp optimization (PSO) [25]. These optimization methods however might not provide the best predicted response, and this can be attributed to different sources of uncertainties as well as inherent error in the model which could lead to good performance for a set of parameters yet poor performance for validation.

3.1 Generalized Likelihood Uncertainty Estimation (GLUE)

The GLUE method was initially introduced partly to allow for the possible equifinality of parameter sets during the estimation of model parameters in over-parameterized models. Based on the estimation of the weights or probabilities associated with different parameter sets using a subjective likelihood measure, the GLUE method derives a posterior probability function and subsequently applies it for the prediction of probability of the output variables. The popularity of GLUE can be attributed to its conceptual simplicity and relative ease of implementation, requiring no modifications to existing source codes of simulation [26]. When applying the GLUE method for uncertainty analysis, the Monte Carlo simulation is used to generate multiple sets of model parameters. Prior distributions are often assumed since these parameter-specific probability density functions

(PDFs) are unknown before the uncertainty analysis. In this study, the prior distributions of the parameters are assumed to be uniform and a traditional likelihood measure for model efficiency and coefficient of determination is selected, which is defined as

$$L = -G\,log\{\mathrm{Var}[E(\theta)]\} \tag{4}$$

where L is the likelihood function; θ represents the parameter set; $E(\theta)$ is the error between observation and model output for the time duration under investigation; G is the shaping factor; $Var(E(\theta))$ is the variance of error; and *log* is the natural logarithmic. For large values of G close to infinite, all weight will be on the single best simulation while all simulations will tend to have equal weight for small values of G [26]. In this study, a series of candidate values are tested including 2^{13}, 2^{12}, 2^{11}, 2^{10}, 2^9, 2^8, 2^7, 2^6 (which are referred to hereafter as G_1 to G_8, respectively) to identify appropriate value of G for the uncertainty analysis. A recently developed Markov Chain Monte Carlo sampler namely DREAM (ZS) (Differential Evolution Adaptive Metropolis algorithm) is also used in this study [27].

Table 3. Parameter bounds for uncertainty analysis

parameter	β_1 (N/s^2)	$\alpha_1\beta_0$ (N/ms^2)	α_2 (N/m)	α_3 (N·m)
Upper bound	4×10^2	2×10^{10}	1×10^7	1×10^2
Lower bound	0	0	0	0

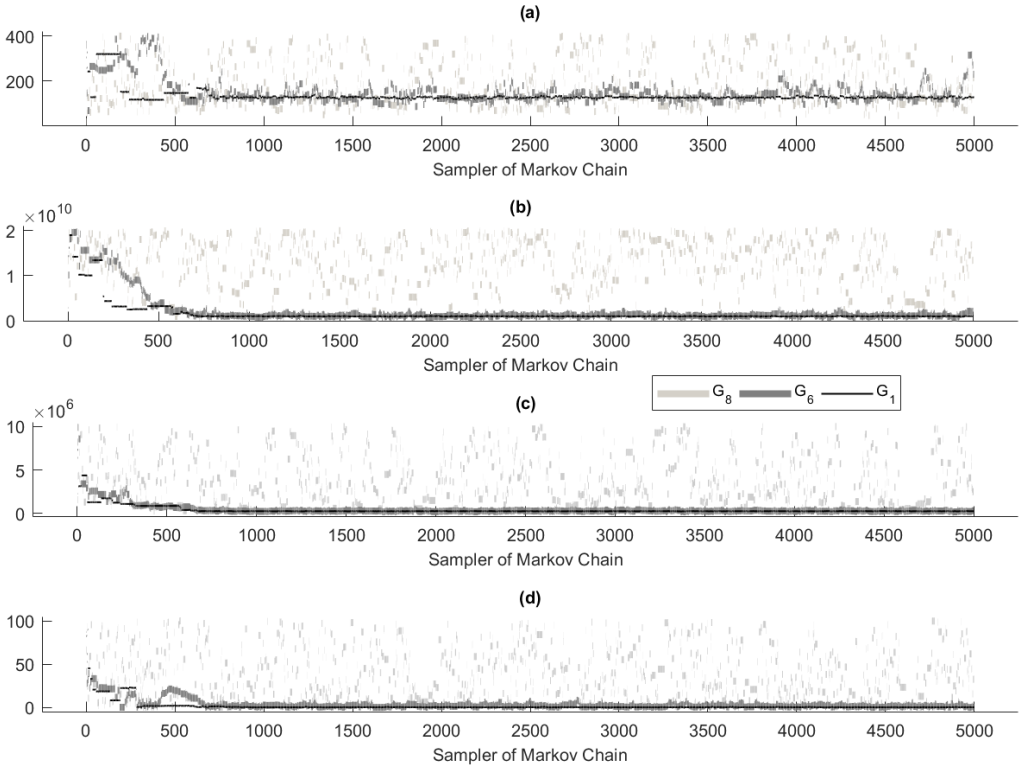

Figure 5. Posterior parameter distributions for (a) β_1; (b) $\alpha_1\beta_0$; (c) α_2; (d) α_3 with G_1, G_6 and G_8

3.2 Effect of Shaping Factor G on Convergence

As indicated previously, a series of candidate values of G are evaluated to select appropriate value for uncertainty analysis. Figure 5 only presents posterior parameter distributions from uncertainty analysis with three selected G values of 2^{13}, 2^8, and 2^6 (i.e., G_1, G_6 and G_8) for the purpose of illustration. The distributions are observed to oscillate between the lower and upper bounds of predefined uniform distributions in Table 3.

The value of *G* is observed to have strong influence on the posterior parameter distributions. For the case of G_8 of 2^6, the Markov Chains can be observed to have continuous oscillation implying unconverged results, while the Markov Chains converge to deterministic values in Table 2 for each individual parameter for the case of G_1 equal to 2^{13} indicating not informative uncertainty analysis results.

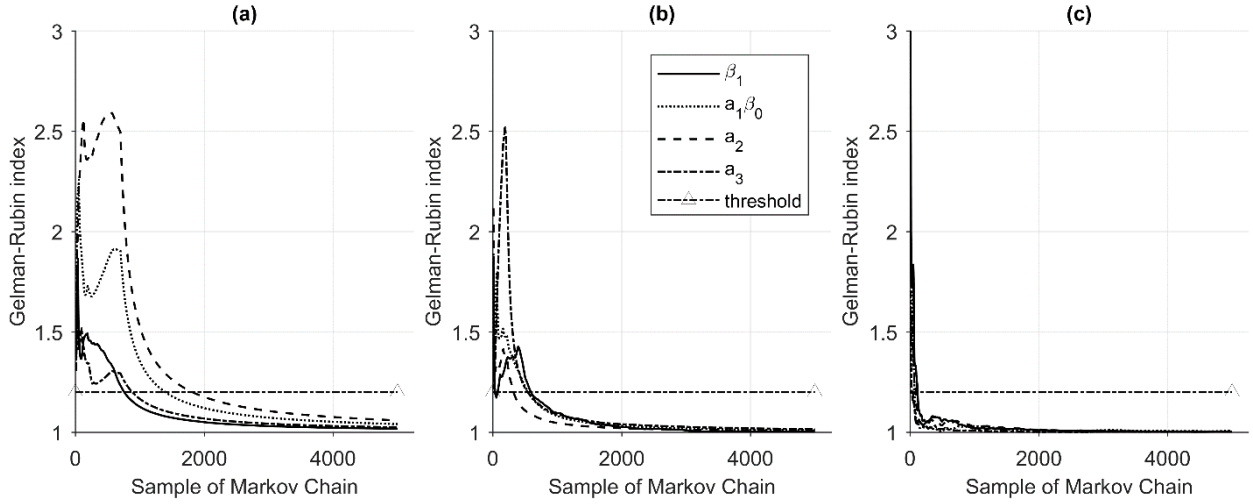

Figure 6 Evolution of the G-R convergence index: (a) G_8; (b) G_6; (c) G_1

To select the appropriate posterior parameter distributions for subsequent analysis, the Gelman-Rubin (G-R) diagnostic [28] is used for convergence check in this study. Figure 6 presents the G-R plots for the Markov Chains from the uncertainty analysis for the case of G_1, G_6 and G_8. The horizontal dashed line represents the threshold value of 1.2 for convergence. Comparing the G-R indices for different G values, it can be observed that it takes longer to reach convergence for small values of *G* and the convergence gets faster with the increase of *G* value.

3.2 Statistics of Probabilistic Model Parameters

Following the above discussion, the posterior parameters from uncertainty analysis with G_6 equal to 2^8 are selected for further analysis. Statistics of the four parameters are summarized in Table 4 including the mean, variance, skewness and the coefficient of variance. All four parameters are observed to have non-zero positive skewness, indicating that these parameters follow distributions other than Gaussian. The parameter α_3 is observed to have the largest coefficient of variance, which indicates that this parameter has the largest uncertainty. In another word, the largest variation of α_3 also implies that the servo-hydraulic model under investigation is least sensitive to α_3. Comparing with the deterministic values in Table 2, it can be observed that there are about 14.3%, 24.8%, 17.4% and 2850% in the mean values in Table 4.

Table 4 Statistics of Servo-hydraulic System Parameters

Parameter	Mean	Standard Deviation	Skewness	Coefficient of Variance
β_1 (N/s^2)	146.27	34.74	1.28	0.24
$\alpha_1\beta_0$ (N/ms^2)	1.26×10^9	3.61×10^8	1.13	0.29
α_2 (N/m)	2.84×10^5	6.38×10^4	0.99	0.23
α_3 (N·m)	1.77	1.52	1.52	0.86

4. Comparison of deterministic and probabilistic models

To illustrate the effect of uncertainties on the servo-hydraulic model, the probabilistic model prediction is compared with that of the corresponding deterministic model. The samples after convergence from uncertainty

analysis are applied for prediction and the resulted predictions are analyzed in both the frequency and time domain. Figure 7 shows the frequency responses of both probabilistic and deterministic models in comparison with the experimental results. Although general good agreement can be observed between the frequency response of the experimental results and that of the corresponding deterministic model, noticeable differences exist such as the amplitude at high frequencies for the test with k=0 kN/m and the phase difference at low frequencies for the test with k=250 kN/m. This can be attributed to the fact that the deterministic model is derived from optimization over the entire frequency range. Using the deterministic model to predict servo-hydraulic actuator response therefore might lead to potential error at some frequencies. On the other hand, the frequency response prediction from the probabilistic model is observed to almost cover the experimental results over the entire range of frequency between 0 and 10 Hz. This indicates that the posterior parameter values can help provide a probabilistic prediction with higher reliability.

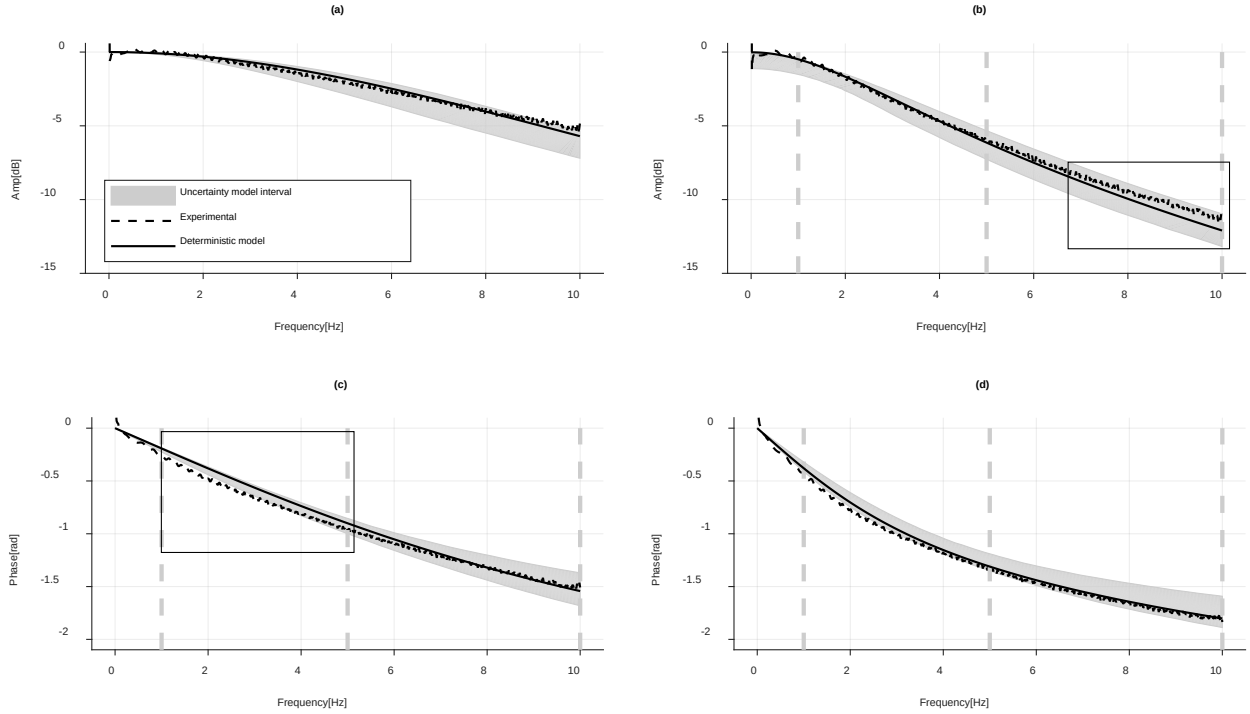

Figure 7. Comparison of frequency responses: (a) and (c) amplitude and phase for test with k=0 kN/m; (b) and (d) amplitude and phase for test with k=250 kN/m

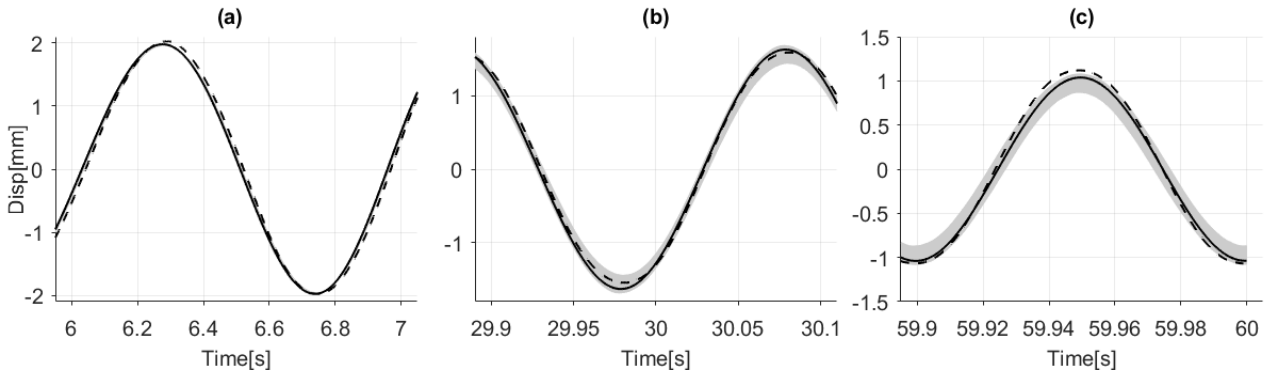

Figure 8. Comparison of displacement prediction between the deterministic and probabilistic models for test with k=0 kN/m: (a) f=1Hz; (b) f=5Hz; (c) f=10Hz;

In order to compare the two models more intuitively, the time-domain prediction is presented in the Figures 8 and 9 at different frequencies around 1.0, 5.0 and 10.0 Hz. It can be observed that most of the experimental observations are within the prediction interval from the probabilistic model. The deterministic model is observed to have better accuracy and reliability at medium and high frequencies than at low frequencies. For the experimental results at low frequencies, the observed values cannot be completely replicated, which indicates that there exists a limit to the model capability, and the uncertainty of the parameters alone is not enough to make up for this deficiency.

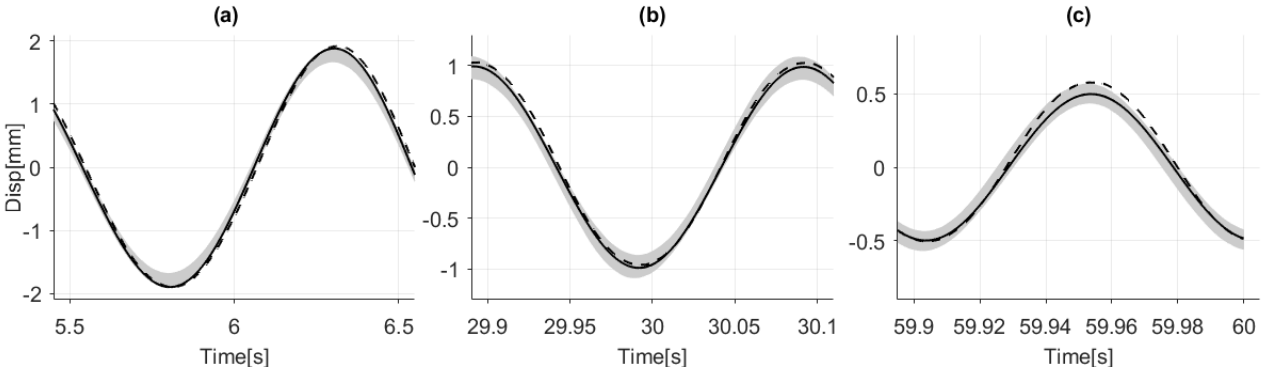

Figure 9. Comparison of displacement prediction between the deterministic and probabilistic models for test with k=250 kN/m: (a) f=1Hz; (b) f=5Hz; (c) f=10Hz

Figures 10 and 11 present the histograms of amplitude and phase responses from the probabilistic model at the frequencies of 1, 5 and 10 Hz for the two tests, respectively. Also presented at the corresponding frequencies in Figures 10 and 11 are the frequency responses from experimental observations and the deterministic model for the purpose of comparison. The probabilistic model is observed to provide a range of predictions, such as from -0.2 to 0.05 dB for the amplitude at frequency of 1 Hz in Figure 10(a) and -1.9 to -1.5 degree for the phase at frequency of 10 Hz in Figure 11(f). Consistent with the time domain analysis results, the phase and amplitude of the experiments are also very close to the deterministic model, and most are enveloped between the upper and lower bounds of the prediction from the probabilistic model.

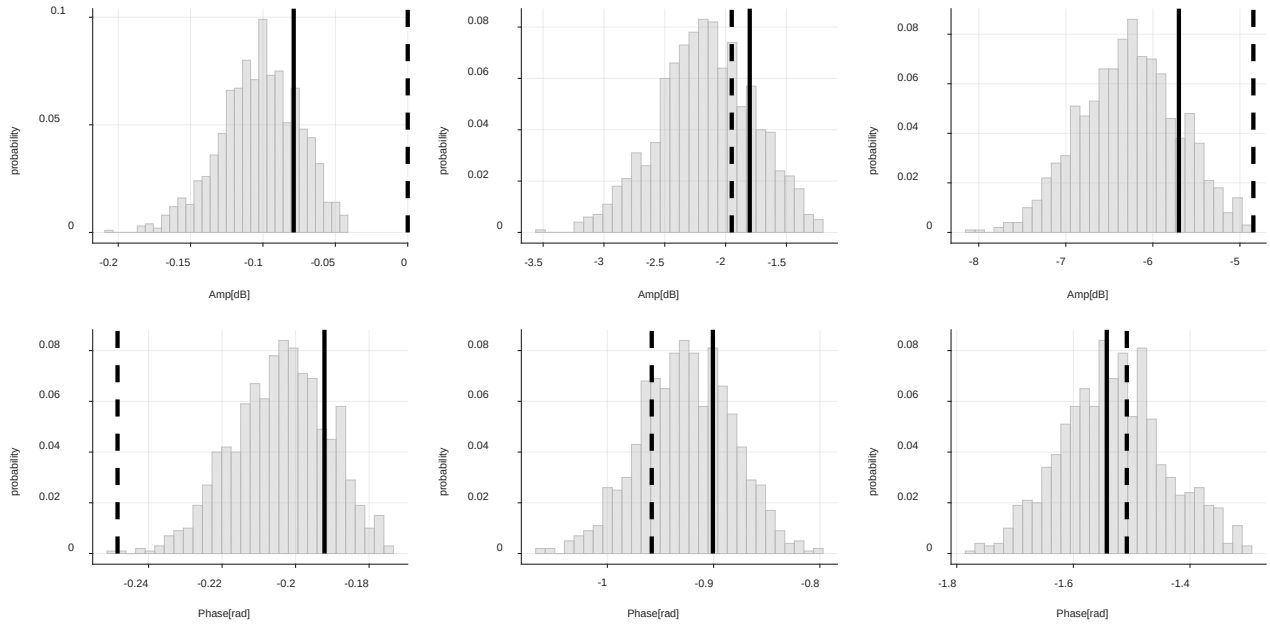

Figure 10. Amplitude and phase response distribution at a single frequency with k=0 kN/m

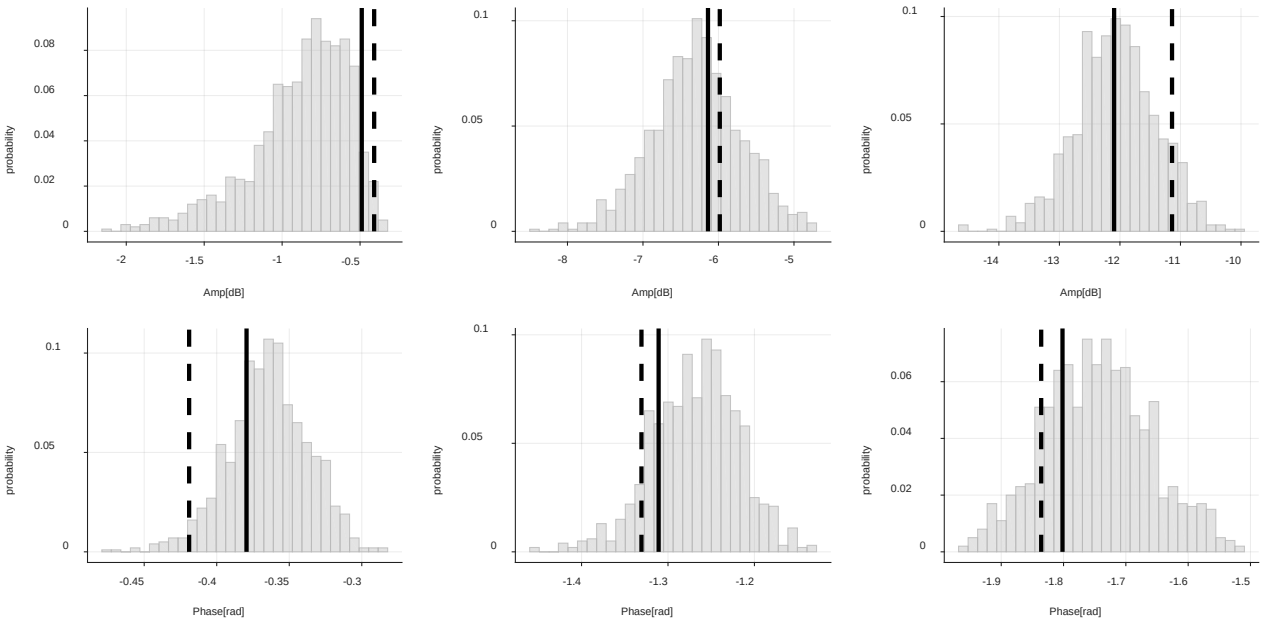

Figure 11. Amplitude and phase response distribution at a single frequency with k=250 kN/m

5. Summary and Conclusion

Uncertainties in servo-hydraulic dynamics not only impacts the stability and performance of controllers designed for accurate actuator control in real-time hybrid simulation but also could affect the experimental design of real-time hybrid simulation to account for structural uncertainties. Based on a commonly used linearized servo-hydraulic system model, this study applies the GLUE method to estimate the probabilistic distribution and statistical moments of the model parameters based on the experiments with different specimens. The derived probabilistic model is then compared with the experimental results and the deterministic model. The probabilistic model is demonstrated to enable better prediction of actuator response through accounting for inherent uncertainties in servo-hydraulic system. The presented probabilistic analysis results can be further applied toward uncertainty analysis of RTHS for engineering research.

6. References

[1] Takanashi K, Ohi K (1983): Earthquake response analysis of steel structures by rapid computer-actuator on-line system: Part I: a progress report, trial system and dynamic response of steel beams. Bulletin of Earthquake Resistant Structure Research Center (ERS), 16, 103–109.

[2] Dermitzakis SN, Mahin SA (1985): Development of substructuring techniques for on-line computer controlled seismic performance testing. Report UCB-EERC-85/04, Earthquake Engineering Research Center, University of California, Berkeley.

[3] Shing PB, Nakashima M, Bursi OS (1996): Application of pseudodynamic test method to structural research. Earthquake Spectra, 12(1), 29–56.

[4] Mosqueda G (2003): Continuous Hybrid Simulation with Geographically Distributed Substructures. PhD Dissertation, Department of Civil and Environmental Engineering, University of California, Berkeley.

[5] Watanabe E., Kitada T., Kunitomo S, Nagata K (2001): Parallel Pseudodynamic Seismic Loading Test on Elevated Bridge System through the Internet. Proceedings of the 8th East Asia-Pacific Conference on Structural Engineering and Construction, Singapore.

[6] Nakashima M, Kato H, Takaoka E (1992): Development of real-time pseudodynamic testing. Earthquake Engineering and Structural Dynamics, 21(1), 79-92.

[7] Blakeborough A, Williams MS, Darby AP, Williams DM (2001): The development of real-time substructure testing. Philosophical Transactions of the Royal Society of London A, 359, 1869-1891.

[8] Chen C, Ricles JM, Marullo, TM and Mercan, O (2009): Real-time hybrid testing using the unconditionally stable explicit CR integration algorithm. Earthquake Engineering and Structural Dynamics, 38(1), 23-44.

[9] Multi-hazard Engineering Collaboratory for Hybrid Simulation (2017): Breaking Barriers & Building Capacity, December 12-13, the University of California, San Diego, http://mechs.designsafe-ci.org

[10] Wallace MI, Sieber J, Neild SA, Wagg DJ, Krauskopf B (2005): Stability analysis of real-time dynamic substructuring using delay differential equation models. Earthquake Engineering and Structural Dynamics, 34, 1817-1832.

[11] Chen C, Ricles JM (2008): Stability analysis of SDOF real-time hybrid testing systems with explicit integration algorithms and actuator delay. Earthquake Engineering and Structural Dynamics, 37, 597-613.

[12] Mercan O, Ricles J M, (2007): Stability and accuracy analysis of outer loop dynamics in real-time pseudodynamic testing of SDOF systems. Earthquake Engineering and Structural Dynamics, 36, 1523-1543.

[13] Huang L, Chen C, Guo T, Chen M (2018): Stability Analysis of Real-Time Hybrid Simulation for Time-Varying Actuator Delay Using the Lyapunov-Krasovskii Functional Approach. Journal of Engineering Mechanics, 145 (1), 04018124, https://doi.org/10.1061/(ASCE)EM.1943-7889.0001550

[14] Horiuchi T, Inoue M, Konno T, Namita Y (1999): Real-time hybrid experimental system with actuator delay compensation and its application to a piping system with energy absorber. Earthquake Engineering and Structural Dynamics, 28(10), 1121-1141.

[15] Chen C and Ricles, JM (2010): Tracking Error-Based Servo-Hydraulic Actuator Adaptive Compensation for Real-Time Hybrid Simulation. Journal of Structural Engineering, 166(4), 485-495.

[16] Phillips BM and Spencer, BF Jr. (2013): Model-Based Feedforward-Feedback Actuator Control for Real-Time Hybrid Simulation. Journal of Structural Engineering, 139, 1205-1214.

[17] Abbiati G, Marelli S, Sudret B, Bursi O, Stojadinovic B (2015): Uncertainty Propagation and Global Sensitivity Analysis in Hybrid Simulation using Polynomial Chaos Expansion. Proceedings of the Fourth International Conference on Soft Computing Technology in Civil, Structural and Environmental Engineering.

[18] Abbiati G, Whyte C, Marelli S, Caracoglia L, Stojadinovic B (2015): Hybrid simulation of uncertainty contaminated structural systems, Proceedings of the Conference of the ASCE Engineering Mechanics Institute.

[19] Chen C, Xu W, Guo T, K. Chen (2017): Analysis of actuator delay and its effect on uncertainty quantification for real-time hybrid simulation. Earthquake Engineering and Engineering Vibration, 16, 713-725.

[20] Silva CE, Gomezb D, Maghareh A, Dyke SJ, and Spencer BF Jr. (2019): Benchmark control problem for real-time hybrid simulation. Mechanical Systems and Signal Processing, 135(1), 106381.

[21] Zhao J, Shield C, French C, Posbergh T (2005): Nonlinear system modeling and velocity feedback compensation for effective force testing. Journal of Engineering Mechanics 131(3), 244-253.

[22] Reinhorn AM, Sivaselvan MV, Weinreber S, and Shao X (2004): A Novel approach for dynamic force control. Proceedings of third European conference on structural control, Vienna university of Technology, Vienna, Austria.

[23] Maghareh A, Silva CE, and Dyke SJ (2018): Servo-hydraulic actuator in controllable canonical form: Identification and experimental validation. Mechanical Systems and Signal Processing, 100, 398-414.

[24] MATLAB. (2019). version R2019a. Natick, Massachusetts: The MathWorks Inc.

[25] Kennedy, J.; Eberhart, R. (1995). "Particle Swarm Optimization". Proceedings of IEEE International Conference on Neural Networks. IV. pp. 1942–1948.

[26] Glue T (1993): The Generalized Likelihood Uncertainty Estimation methodology. Methodology, 53–69.

[27] Vrugt JA (2016): Markov chain Monte Carlo simulation using the DREAM software package: Theory, concepts, and MATLAB implementation. Environmental Modelling and Software, 75, 273-316.

[28] Gelman A, Rubin D (1992): Inference from Iterative Simulation Using Multiple Sequences. Statistical Science, 7(4), 457-472.

